Liquid Crystals

Publication details, including instructions for authors and subscription information:
http://www.informaworld.com/smpp/title~content=t713926090

Liquid crystals derived from 2-phenylisoindoles: synthesis and characterization

Kenny G. Jow; Theo J. Dingemans

To cite this Article Jow, Kenny G. and Dingemans, Theo J.(2002) 'Liquid crystals derived from 2-phenylisoindoles: synthesis and characterization', Liquid Crystals, 29: 4, 573 — 581
To link to this Article: DOI: 10.1080/02678290110116213
URL: http://dx.doi.org/10.1080/02678290110116213

LIQUID CRYSTALS, 2002, VOL. 29, NO. 4, 573–581

Taylor & Francis
Taylor & Francis Group

Liquid crystals derived from 2-phenylisoindoles: synthesis and characterization

KENNY G. JOW
Department of Materials Science and Engineering,
Massachusetts Institute of Technology, 77 Massachusetts Avenue, Cambridge,
MA 02139-4307, USA

and THEO J. DINGEMANS*
ICASE, Mail Stop 132C, 3 West Reid Street, NASA Langley Research Center,
Hampton, VA 23681-2199, USA

(*Received 21 August 2001; accepted 26 October 2001*)

2-Phenylisoindole was investigated as the rigid core unit in a series of asymmetric mesogenic molecules. When the 2-phenylisoindole core was terminated with a hexyl tail, no mesophase formation could be observed. When 4-*n*-(tridecafluorohexyl) was used, however, both monotropic and enantiotropic phase behaviour were observed. It was found that most functionalities at the anhydride 5-position results in the formation of smectic A (SmA) phases in the temperature range 70–180°C. Functionalities at the anhydride 4-position suppress mesophase formation. Large substituents (−Br, $-NO_2$) and symmetric substitution patterns (5,6-dichloro, 4,7-dichloro and 4,5,6,7-tetrachloro) on the anhydride moiety increase the melting point and destabilize the mesophase. Temperature dependent X-ray diffraction experiments suggest an interdigitated SmA packing for this family of compounds.

1. Introduction

Fluorinated polyimides are well known for their mechanical properties, thermal stability, and ability to survive in aggressive environments [1]. Currently, very few examples exist in which imides are used as mesogenic building blocks in low molar mass thermotropic liquid crystals (LCs) of the 'core–tail' type. Eiselt and co-workers [2] reported a series of LC di-imides based on 3,3′,4,4′-biphenyltetracarboxylic dianhydride (BPDA) as the central mesogenic core. They concluded that the dianhydride core adopts the *trans*-configuration when reacted with 4-*n*-alkylanilines or 4-*n*-alkoxyanilines, and they exclusively observed the SmA phase in the temperature range 226–293°C. Bialecka-Florjańczyk and Orzeszko [3] reported the synthesis of a series of monothio- and dithio-trimellitimides. Nematic and smectic phases were observed in the 4-cyano substituted compounds, whereas only a nematic mesophase was observed in the 4-decyloxy analogue. Transition temperatures for these compounds were reported to be in the range 49–203°C. Most recently Berdagué *et al.* [4] showed that 2-phenylindazole can be used as a mesogenic building block for LCs and reported the existence of both nematic and smectic mesophases.

Herein, we present the synthesis and characterization of new imide-based LCs prepared from simple anhydrides and 4-*n*-tridecafluorohexylaniline. This class of heterocyclic compounds is better known as the 2-phenylisoindole-1,3-diones; they have an asymmetric calamitic rigid core structure (shown below) that is conducive to mesophase formation.

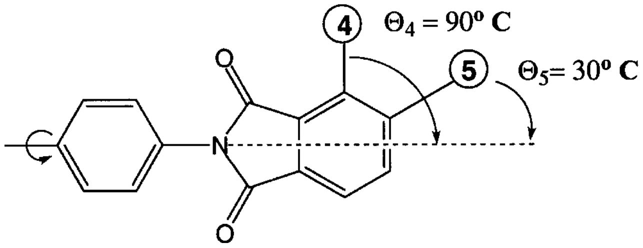

Potential substituents on the anhydride moiety have to be considered as lateral substituents because no *para*-position is available and, depending on the position, they are placed at a 90° angle (4-position) or at a 30° angle (5-position) with respect to the molecular long axis. Our main interests were to examine the effects of

---

*Author for correspondence;
e-mail: t.j.dingemans@larc.nasa.gov

Liquid Crystals ISSN 0267-8292 print/ISSN 1366-5855 online © 2002 Taylor & Francis Ltd
http://www.tandf.co.uk/journals
DOI: 10.1080/02678290110116213

the anhydride substituents on mesophase type and mesophase stability in a series of 2-phenylisoindole-based model compounds.

In the first series we modified 2-(4-*n*-tridecafluorohexylphenyl)isoindole-1,3-dione (**1**) by introducing simple substituents (X = H, Me, OMe, and NO_2) at the anhydride 5-position (**I**). Most anhydrides were commercially available or could be made in one or two steps.

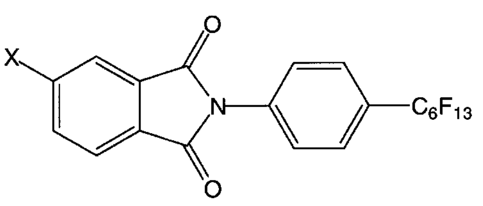

(**I**) X= H, Me, OMe, NO_2

Next, we considered 2-(4-*n*-tridecafluorohexylphenyl)-isoindole-1,3-dione (**1**) with different halogen substituents (X = F, Cl, Br) and studied the phase behaviour when the halogens were moved from the anhydride 5-position to the 4-position (**II**). By doing so, we reduced the mesogen effective length (i.e. lowered the symmetry) and in addition placed the electrostatic dipole moment at a 90° angle with respect to the molecular long axis.

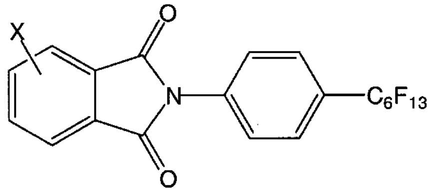

(**II**) X= 4-F, 4-Cl, 4-Br and 5-F, 5-Cl, 5-Br

Finally, in the last series (**III**) we explored the effects of multiple halogen (X = Cl) substitutions on the terminal anhydride moiety of 2-(4-*n*-tridecafluorohexylphenyl)-isoindole-1,3-dione (**1**). The mono-substituted analogues, with chlorine in the 4- or 5-position, are asymmetric, whereas the di- and tetra-substituted analogues are symmetric.

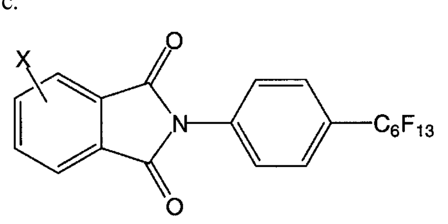

(**III**) X= 4,7-dichloro, 5,6-dichloro and 4,5,6,7-tetrachloro

2. Results and discussion

The three series of 2-phenylisoindole-based thermotropic liquid crystals were successfully synthesized in high yields, using a simple one-step procedure. The structures of all compounds were confirmed by proton, carbon, and fluorine nuclear magnetic resonance ($^1H/^{13}C/^{19}F$ NMR) and infrared spectroscopy (FTIR). Although we initially included 4-hexylaniline in this study, we could detect no liquid crystalline behaviour in any of these systems. This observation suggests that the rigid 2-phenylisoindole core by itself exhibits poor mesogenic properties. We were more successful on switching from 4-hexylaniline to 4-*n*-tridecafluorohexylaniline as the terminal tail segment. As Bunn and Houwens [5] showed, the larger fluorine atoms force a helicoidal chain conformation, and this results in a stiffer chain than in its hydrocarbon analogue. In addition, the fluorinated tail is chemically incompatible with the aromatic 2-phenylisoindole core, which leads to microphase separation and consequently promotes the formation of smectics [6–8].

2.1. *Mesomorphic properties*

The phase behaviour and DSC results of the first series of 5-substituted 2-(4-*n*-tridecafluorohexylphenyl)-isoindole-1,3-diones are presented in table 1.

From these results it is evident that the parent compound 2-(4-*n*-tridecafluorohexylphenyl)isoindole-1,3-dione (**1**) is a poor mesogen. This compound shows a monotropic SmA phase upon cooling only. When lateral substituents are introduced at the anhydride 5-position, X = Me (**2**) and OMe (**3**), an enantiotropic SmA phase is observed that is stable over a wide temperature range. Figure 1 shows a DSC heating and cooling scan of 5-methoxy-2-(4-*n*-tridecafluorohexylphenyl)isoindole-1,3-dione (**3**). Upon heating, this compound shows a

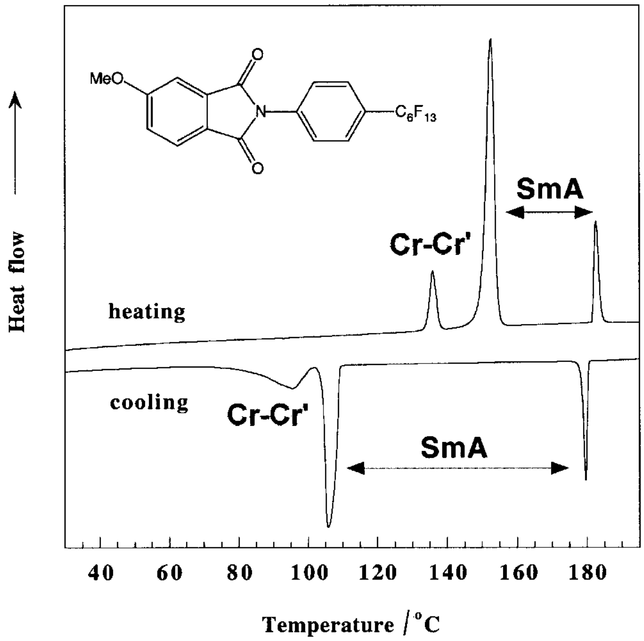

Figure 1. Second heating and cooling trace of 5-methoxy-2-(4-*n*-tridecafluorohexylphenyl)isoindole-1,3-dione.

Table 1. Phase transition temperatures (°C) and enthalpies (kJ mol^{-1}, in brackets) for 5-substituted 2-(4-*n*-tridecafluorohexylphenyl)isoindole-1,3-diones.

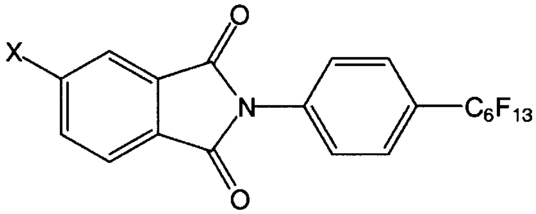

Compound	*X*	Cr		Cr′		SmA		I
1	H	•	140.1(35.1)					•
		•	103.5(−27.0)			•	131.6(−4.0)	•
2	Me	•	145.1(50.6)			•	165.2(9.2)	•
		•	102.0(−44.8)			•	164.7(−9.2)	•
3	OMe	•	133.8(5.5)	•	149.9(34.9)	•	181.5(6.1)	•
		•	100.2(−8.6)	•	109.2(−21.0)	•	180.6(−6.2)	•
4	NO_2	•	147.5(3.4)	•	179.2(42.6)			•
		•	155.0(−40.5)					•

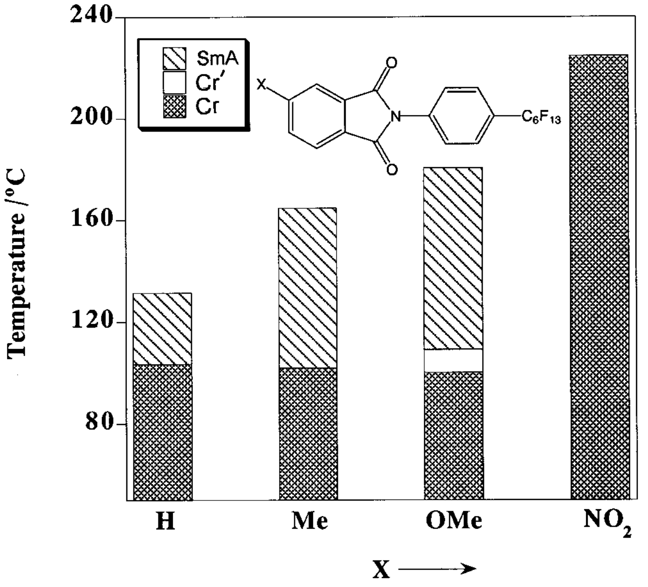

Figure 2. Mesophase ranges for the 5-substituted 2-(4-*n*-tridecafluorohexylphenyl)isoindole-1,3-diones.

SmA phase in the range 150–182°C, but upon cooling, the SmA range extends over 70°C (109–181°C). This supercooling behaviour is typically observed for all mesogenic 2-phenylisoindoles used in this study.

When a nitro group ($X = NO_2$) (**4**) is introduced, no mesomorphic behaviour is observed. This is quite surprising, because the nitro functionality is a highly polarizable group and is often found to promote mesophase formation [9]. In this case, however, we believe that the large planar nitro group promotes crystallization, which results in a high melting temperature obscuring the underlying LC phase. The phase behaviour of the 5-substituted 2-(4-*n*-tridecafluorohexylphenyl)isoindole-1,3-diones is summarized in figure 2, in which the compounds are arbitrarily plotted on the *X*-axis.

The DSC results for the halogen-modified 2-(4-*n*-tridecafluorohexylphenyl)isoindole-1,3-diones are summarized in table 2.

Introducing halogens at the anhydride 5-position, initially results in an increase in melt transition and stabilization of the SmA phase as a function of increasing halogen size for $X = F$ (**6**) and Cl (**8**). When $X = Br$ (**10**), however, the stability of the SmA phase is slightly reduced, probably because the larger halogen size in this case promotes crystallization.

When the halogens ($X = F$, Cl and Br) are moved from the anhydride 5-position to the 4-position, we observe a dramatic reduction of melting temperature for all three compounds. In addition, it is interesting to see that the SmA phase is completely suppressed in the 4-F (**5**) and 4-Br (**9**) isomers (though not in the 4-Cl (**7**) isomer). Intuitively, one would expect to see little or no change in phase behaviour between the 4-F and 5-F isomers because moving the small fluorine atom from the 5- to the 4-position does not significantly affect the overall molecular shape. Translating the bulky chlorine and bromine atoms from the 5- to the 4-position, however, reduces the overall molecular symmetry and results in a considerable drop in melt transition. At this moment we are unable to explain why only the 4-Cl isomer (**7**)

Table 2. Phase transition temperatures (°C) and enthalpies (kJ mol^{-1}, in brackets) for mono-halogenated 2-(4-*n*-tridecafluorohexylphenyl)isoindole-1,3-diones.

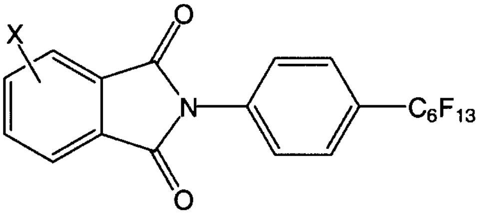

Compound	*X*	Cr		Cr′		SmA		I
5	4-F	•	158.1(40.4)					•
		•	127.5(−26.2)					•
6	5-F	•	126.4(26.9)			•	137.5(4.9)	•
		•	101.8(−25.0)			•	136.5(−4.9)	•
7	4-Cl	•	111.0(26.6)					•
		•	69.8(−16.4)			•	85.3(−1.6)	•
8	5-Cl	•	143.9(3.2)	•	155.2(25.4)	•	164.8(6.5)	•
		•	128.7(−22.2)			•	163.6(−6.7)	•
9	4-Br	•	116.4(32.2)					•
		•	82.9(−17.5)					•
10	5-Br	•	174.0(38.8)					•
		•	141.6(−30.1)			•	164.7(−6.2)	•

exhibits a LC phase. The phase behaviour of the halogen-modified 2-(4-*n*-tridecafluorohexylphenyl)isoindole-1,3-diones is summarized in figure 3.

We also investigated the effects of multi-halogenation on the phase behaviour of 2-(4-*n*-tridecafluorohexylphenyl)-isoindole-1,3-dione model compounds. The DSC results are shown in table 3.

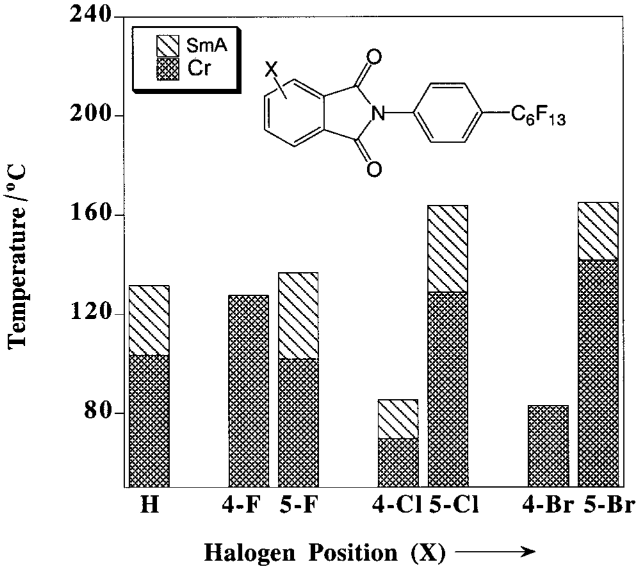

Figure 3. Mesophase ranges for the mono-halogenated 2-(4-*n*-tridecafluorohexylphenyl)isoindole-1,3-diones.

Introducing more than one chlorine atom results in a dramatic loss of mesophase stability. Figure 4 shows the phase behaviour of all chlorine ($X = \mathrm{Cl}$) modified mesogens. We were surprised to see that the isotropization temperatures of the 5-Cl (**8**) and 5,6-Cl (**11**) mesogens are very similar. Placing two chlorine atoms at the anhydride 5- and 6-position increases the strength of the molecular dipole in the direction of the molecular long axis, which would promote mesophase stability. In this case, however, the two chlorine atoms also increase the overall molecular symmetry and this promotes crystallization, which is confirmed by the higher melting point of this compound. The result is a small monotropic SmA phase that could be observed only upon cooling. When the chlorine atoms are placed at the anhydride 4- and 7-position (**12**) the same trend is observed as for the 4-Cl (**7**) compound. In the 4,7-Cl compound we found no mesophases, but again a significant decrease in melting point was observed. It is clear that placing substituents on the 4- and 7-positions results in a reduction of the aspect ratio of the molecule and therefore a reduction in mesophase stability. Perchlorination of the anhydride moiety, as in the case of the 4,5,6,7-Cl compound (**13**), leads to a highly symmetric compound with a very high melting point and exhibiting no mesophase. Again, the high symmetry of this compound seems to favour crystallization over mesophase formation.

Table 3. Phase transition temperatures (°C) and enthalpies (kJ mol^{-1}, in brackets) for multi chlorinated 2-(4-*n*-tridecafluorohexylphenyl)isoindole-1,3-diones.

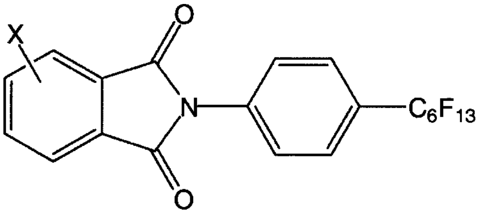

Compound	*X*	Cr		Cr′		SmA		I
11	5,6-Cl	●	186.4(40.7)					●
		●	167.3(−34.0)			●	169.0[a]	●
12	4,7-Cl	●	140.0(18.4)	●	144.2(19.9)			●
		●	102.2(−30.3)					●
13	4,5,6,7-Cl	●	239.6(45.1)					●
		●	220.2(−42.6)					●

[a] Observed by optical microscopy only.

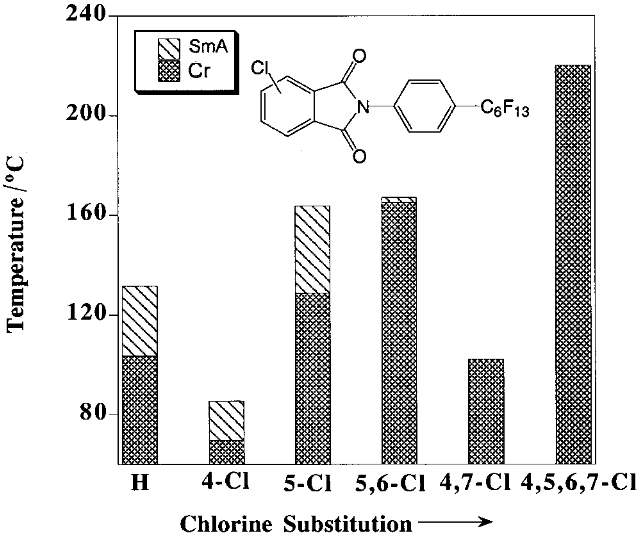

Figure 4. Mesophase ranges for the mono-, di- and tetra-chlorinated 2-(4-*n*-tridecafluorohexylphenyl)isoindole-1,3-diones.

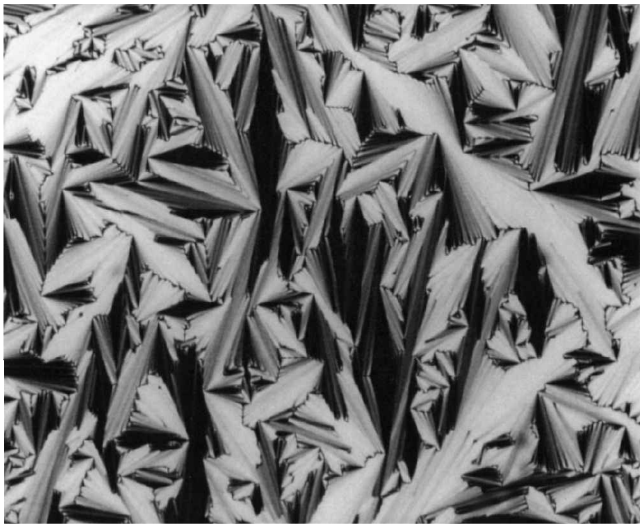

Figure 5. Smectic A focal conic texture of 5-methoxy-2-(4-*n*-tridecafluorohexylphenyl)isoindole-1,3-dione at 160°C; crossed polarizers and 20X.

2.2. *Optical microscopy*

All reported mesogenic compounds exhibit a classical focal-conic texture, which is indicative of the smectic A phase (SmA). Figure 5 shows the texture of 5-methoxy-2-(4-*n*-tridecafluorohexylphenyl)isoindole-1,3-dione (**3**) in the SmA phase at 160°C.

2.3. *X-ray diffraction*

Figure 6 shows the X-ray diffractogram of 5-methoxy-2-(4-*n*-tridecafluorohexylphenyl)isoindole-1,3-dione (**3**) in the unaligned SmA phase at 160°C. Attempts to orient samples in the SmA phase using a strong magnetic field were unsuccessful. This diffraction pattern is representative for all mesogens and appears to be temperature independent.

The broad peak at the wide angle region ($2\theta \sim 16°$) is indicative of liquid-like in-plane order of the mesogens within the layers, which is typically observed for lower order smectic phases. The small angle reflection ($2\theta \sim 2.5°$) corresponds to a layer spacing (d) of ~ 34 Å. The molecular length (l) of this mesogen in its most extended conformation is 18.1 Å as estimated by *Spartan*, and is confirmed by the (0 0 1) and (0 0 2) reflections in the crystalline phase. Based on these results we believe

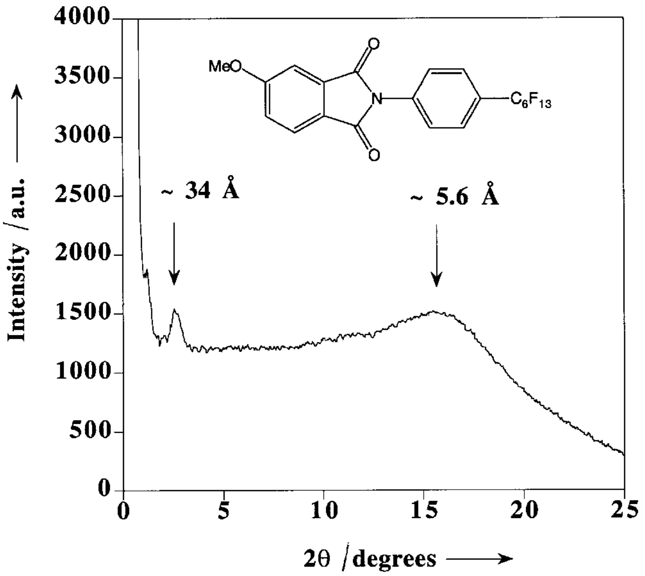

Figure 6. X-ray diffractogram of 5-methoxy-2-(4-*n*-tridecafluorohexylphenyl)isoindole-1,3-dione in the smectic A phase at 160°C.

that our data suggest a bilayer SmA packing model with interdigitating fluorinated tails as presented in figure 7.

3. Conclusions

We are currently investigating low molecular mass imides with perfluorinated tails for applications such as self-adaptive optics and filters. Potential candidates, however, need to withstand extreme temperature fluctuations, the presence of atomic oxygen, and high energy radiation conditions. Most thermotropic LCs rely on alkyl-type flexible tails, but in our applications alkyl groups do not have the required long term stability. We are, therefore, exploring the possibility of using low molecular mass imides with perfluorinated tails. We have synthesized and compared several series of 2-(4-*n*-tridecafluorohexylphenyl)isoindole-1,3-dione liquid crystals. We have found that 2-(4-*n*-tridecafluorohexylphenyl)isoindole-1,3-dione-based liquid crystals are able to form stable SmA phases with accessible temperature ranges (70–180°C). Although many different functionalities are tolerated at the anhydride 5-position, substituents at the anhydride 4-position and multiple halogen substitutions destabilize the SmA phase. X-ray diffraction experiments suggest an interdigitated bilayer SmA packing for this family of compounds.

4. Experimental

4.1. *Instrumentation*

The structures of the final products were confirmed using ^{1}H NMR, ^{13}C NMR, and ^{19}F NMR spectroscopy. The spectra were recorded using a Bruker Avance 300 spectrometer (300 MHz), and infrared spectra were collected using a Nicolet Magna-IR Spectrometer 750.

Transition temperatures were determined using a Perkin Elmer Pyris differential scanning calorimeter, calibrated with indium (99.99%) (m.p. 156.5°C, $\Delta H = 28.315$ J g^{-1}) and tin (99.99%) (m.p. 232.0°C, $\Delta H = 54.824$ J g^{-1}). Heating and cooling scans were recorded at 10°C min^{-1}. Mesophases were identified with an Olympus BH-2 optical microscope, equipped with a Mettler Toledo FP82H hot stage. Samples were examined between glass microscope slides.

Variable temperature X-ray diffraction analysis was carried out with an Enraf Nonius FR 590 system equipped with a two-dimensional image plate detector, 2500 × 2500 pixels, 80 μm resolution. Unaligned samples were analysed using monochromatic Cu-K$_\alpha$ ($\lambda = 1.54$ Å) radiation at various temperatures. A Mettler Toledo FP82H hot stage was used to control the temperature.

4.2. *Materials*

All starting materials were obtained from Aldrich, with the exception of 1-iodotridecafluorohexane, 4-iodoaniline (Fluka), and 4-chlorophthalic anhydride (TCI). Both 3-bromophthalic anhydride and 4-methoxyphthalic anhydride were synthesized according to a procedure reported by Soucy *et al.* [10], and 4-*n*-(tridecafluorohexyl)aniline was prepared according to Yoshino *et al.* [11].

All LC model compounds were synthesized as outlined in the scheme. The amic acid intermediate was formed in the initial room temperature step; when the temperature was raised to reflux, the amic acid was dehydrated to the corresponding imide. Although the reaction appeared to be finished after four hours (TLC 90/10 hexane/ethyl acetate), we heated the reaction mixture under reflux overnight for convenience. This procedure is simple, and gave the desired products in high yields; they often crystallized from the reaction mixture upon cooling, minimizing product work-up.

4.3. *Synthesis*

4.3.1. *3-Bromophthalic anhydride*

A three-neck flask equipped with a magnetic stirrer and reflux condenser was charged with 3-bromo-*o*-xylene (3 g, 0.016 mol), cetyltrimethylammonium bromide (0.01 g, 0.03 mmol) and 60 ml water. Potassium permanganate (10 g, 0.063 mol) was added in three portions and the reaction mixture was stirred at 60°C for 24 h. The warm reaction mixture was filtered and the filtrate acidified with 10 ml HCl (37%). The volume was reduced to 50% and extracted with diethyl ether (3x); the combined ether layers were dried over $MgSO_4$. The solvent was removed by distillation and an off-white product collected and heated under reflux in acetic anhydride for 4 h. Upon cooling, colourless crystals formed. Yield 1.81 g

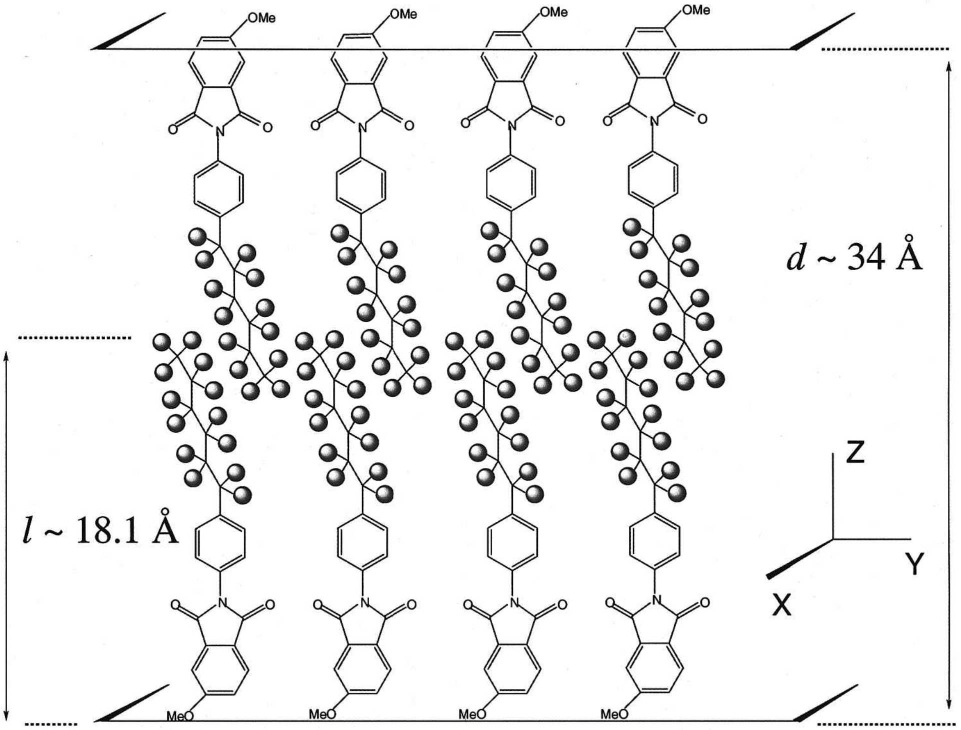

Figure 7. Proposed bilayer packing of 5-methoxy-2-(4-*n*-tridecafluorohexylphenyl)isoindole-1,3-dione in the smectic A phase with interdigitating fluorinated tails.

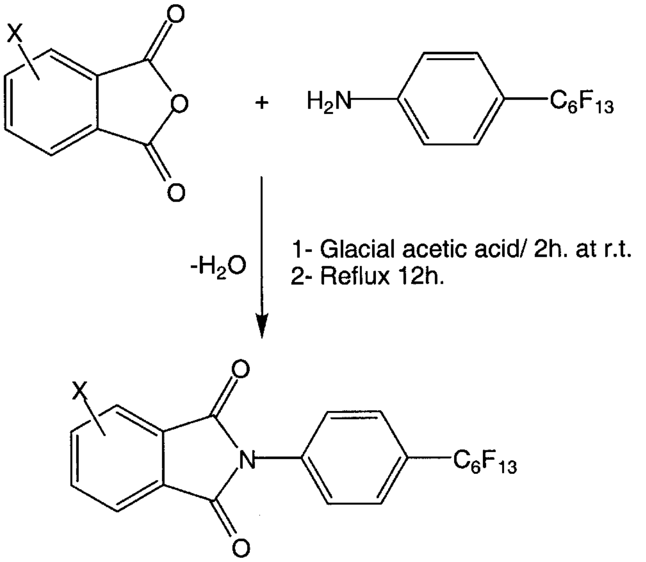

Scheme. Synthesis of the 2-phenylisoindole model compounds.

(50%), m.p. 135°C (m.p. 134°C [10]). FTIR (KBr) 1772 ($C{=}O_{anhydride}$), 1858 ($C{=}O_{anhydride}$) cm^{-1}.

4.3.2. *4-Methoxyphthalic anhydride*

The same procedure was used as described for 3-bromophthalic anhydride. Oxidation was complete after 5 h. Yield 4 g (35%), m.p. 95°C (95°C [10]). FTIR (KBr) 1774 ($C{=}O_{anhydride}$), 1847 ($C{=}O_{anhydride}$) cm^{-1}.

4.3.3. *4-n-(Tridecafluorohexyl)aniline*

A 250 ml two-neck flask equipped with reflux condenser and nitrogen inlet was charged with 1-iodotridecafluorohexane (67.9 g, 0.152 mol), 4-iodoaniline (30.0 g, 0.137 mol), copper bronze (29.0 g, 0.456 mol) and 150 ml DMSO. This suspension was heated at 120°C for 12 h under a nitrogen atmosphere. The reaction mixture was cooled to 50°C and the copper iodide and excess copper bronze were removed by vacuum filtration. Water (100 ml) was added to the filtrate and the aqueous layer was extracted (3x) with diethyl ether. The ether layer was washed with water, dried over $MgSO_4$ and the solvent removed by distillation. The title compound was purified by vacuum distillation (60°C/25 mTorr). Yield 37.5 g (61%). ^1H NMR ($CDCl_3$) δ (ppm): 3.85 (s, 2H), 6.57 (d, 2H, $J = 9$ Hz), 7.23 (d, 2H, $J = 8$ Hz). ^{13}C NMR ($CDCl_3$) δ (ppm): 114.23, 117.77, 118.03, 128.19, 128.27, 128.36, 149.73. ^{19}F NMR ($CDCl_3$) δ (ppm): -82 (ω-C$\underline{F}_3$), -110 (ε-C$\underline{F}_2$), -122 (δ-C$\underline{F}_2$), -123 (γ-C$\underline{F}_2$), -125 (β-C$\underline{F}_2$), -127 (α-C$\underline{F}_2$).

4.3.4. *Representative procedure for the synthesis of 2-(4-n-tridecafluorohexylphenyl)isoindole-1,3-dione (1)*

A 50 ml one-neck flask equipped with a magnetic stirrer bar and reflux condenser was charged with phthalic anhydride (0.441 g, 3 mmol), 4-*n*-(tridecafluorohexyl)aniline (1.44 g, 3.5 mmol) and 20 ml glacial acetic acid. This mixture was stirred for 2 h at room temperature followed by heating at reflux (12 h). Upon cooling, colourless crystals formed which were collected by filtration and recrystallized once more from ethanol. Yield 1.44 g (89%), $t_r = 0.3$. ^{1}H NMR (CDCl$_3$) δ (ppm): 7.67 (d, 2H, $J = 8$ Hz), 7.73 (d, 2H, $J = 9$ Hz), 7.81 (t, $J = 3$ Hz, 1H), 7.82 (s, 1H), 7.95 (s, 1H), 7.97 (t, $J = 3$ Hz, 1H). ^{13}C NMR (CDCl$_3$) δ (ppm): 123.9, 126, 127.6, 127.7, 131.3, 134.6, 135.1, 166.5. ^{19}F NMR (CDCl$_3$) δ (ppm): −81 (ω-C$\underline{F}_3$), −111 (ε-C$\underline{F}_2$), −122 (δ, γ-C$\underline{F}_2$), −123 (β-C$\underline{F}_2$), −126 (α-C$\underline{F}_2$). FTIR (KBr): 1717 (C=O$_{imide}$), 1782 (C=O$_{imide}$) cm^{-1}.

4.3.5. *Analytical data for 5-methyl-2-(4-n-tridecafluorohexylphenyl)isoindole-1,3-dione (**2**)*

Yield 1.45 g (87%), $t_r = 0.18$. ^{1}H NMR (CDCl$_3$) δ (ppm): 2.55 (s, 3H), 7.59 (d, 1H, $J = 7$ Hz), 7.66 (d, 2H, $J = 9$ Hz), 7.71 (d, 2H, $J = 9$ Hz), 7.76 (s, 1H), 7.84 (d, 1H, $J = 7$ Hz). ^{13}C NMR (CDCl$_3$) δ (ppm): 22.6, 123.7, 124.3, 125.9, 127.4, 127.5, 127.6, 128.7, 131.6, 135.1, 146, 166.5, 166.6. ^{19}F NMR (CDCl$_3$) δ (ppm): −81 (ω-C$\underline{F}_3$), −111 (ε-C$\underline{F}_2$), −122 (δ, γ-C$\underline{F}_2$), −123 (β-C$\underline{F}_2$), −127 (α-C$\underline{F}_2$). FTIR (KBr): 1726 (C=O$_{imide}$), 1781 (C=O$_{imide}$) cm^{-1}.

4.3.6. *Analytical data for 5-methoxy-2-(4-n-tridecafluorohexylphenyl)isoindole-1,3-dione (**3**)*

Yield 1.61 g (94%), $t_r = 0.16$. ^{1}H NMR (CDCl$_3$) δ (ppm): 3.95 (s, 3H), 7.25 (dd, 1H, $J = 6$ Hz), 7.42 (d, 1H, $J = 3$ Hz), 7.65 (d, 2H, $J = 9$ Hz), 7.71 (d, 2H, $J = 8$ Hz), 7.86 (d, 1H, $J = 8$ Hz). ^{13}C NMR (CDCl$_3$) δ (ppm): 54.1, 56.2, 108.3, 120.7, 123.2, 125.6, 125.9, 127.6, 134, 135.3, 165.1, 166.2, 166.4. ^{19}F NMR (CDCl$_3$) δ (ppm): −81 (ω-C$\underline{F}_3$), −111 (ε-C$\underline{F}_2$), −122 (δ, γ-C$\underline{F}_2$), −123 (β-C$\underline{F}_2$), −127 (α-C$\underline{F}_2$). FTIR (KBr): 1718 (C=O$_{imide}$), 1782 (C=O$_{imide}$) cm^{-1}.

4.3.7. *Analytical data for 5-nitro-2-(4-n-tridecafluorohexylphenyl)isoindole-1,3-dione (**4**)*

Yield 1.32 g (75%), $t_r = 0.25$. ^{1}H NMR (CDCl$_3$) δ (ppm): 7.67 (d, 2H, $J = 8$ Hz), 7.76 (d, 2H, $J = 9$ Hz), 8.18 (d, 1H, $J = 8$ Hz), 8.69 (dd, 1H, $J = 2$ Hz), 8.78 (d, 1H, $J = 2$ Hz). ^{13}C NMR (CDCl$_3$) δ (ppm): 118.0, 123.9, 124.6, 126.6, 127.4, 128.5, 131.4, 133.0, 134.3, 150.7, 162.9, 163.2. ^{19}F NMR (CDCl$_3$) δ (ppm): −81 (ω-C$\underline{F}_3$), −111 (ε-C$\underline{F}_2$), −122 (δ, γ-C$\underline{F}_2$), −123 (β-C$\underline{F}_2$), −126 (α-C$\underline{F}_2$). FTIR 1717 (KBr): (C=O$_{imide}$), 1780 (C=O$_{imide}$) cm^{-1}.

4.3.8. *Analytical data for 4-fluoro-2-(4-n-tridecafluorohexylphenyl)isoindole-1,3-dione (**5**)*

Yield 1.54 g (92%), $t_r = 0.11$. ^{1}H NMR (CDCl$_3$) δ (ppm): 7.46 (tt, 1H, $J = 2$ Hz), 7.64 (d, 2H, $J = 9$ Hz), 7.72 (d, 2H, $J = 8$ Hz), 7.8 (m, 2H). ^{13}C NMR (CDCl$_3$) δ (ppm): 120, 120.1, 122.7, 123, 126, 127.7, 133.4, 134.6, 137, 137.1, 156, 159.6, 163.1, 165.3. ^{19}F NMR (CDCl$_3$) δ (ppm): −81 (ω-C$\underline{F}_3$), −111 (ε-C$\underline{F}_2$), −112 ($\underline{F}$-Ar), −122 (δ, γ-C$\underline{F}_2$), −123 (β-C$\underline{F}_2$), −127 (α-C$\underline{F}_2$). FTIR (KBr): 1724 (C=O$_{imide}$), 1784 (C=O$_{imide}$) cm^{-1}.

4.3.9. *Analytical data for 5-fluoro-2-(4-n-tridecafluorohexylphenyl)isoindole-1,3-dione (**6**)*

Yield 1.49 g (89%), $t_r = 0.34$. ^{1}H NMR (CDCl$_3$) δ (ppm): 7.48 (tt, 1H, $J = 2$ Hz), 7.64 (m, 1H), 7.65 (d, 2H, $J = 8$ Hz), 7.73 (d, 2H, $J = 8$ Hz) 7.98 (q, 1H, $J = 4$ Hz). ^{13}C NMR (CDCl$_3$) δ (ppm): 111.4, 111.8, 121.6, 121.9, 125.9, 126.3, 126.4, 127.7, 134.1, 134.9, 164.9, 165.2, 165.4, 168.3. ^{19}F NMR (CDCl$_3$) δ (ppm): −81 (ω-C$\underline{F}_3$), −101 ($\underline{F}$-Ar), −111 (ε-C$\underline{F}_2$), −122 (δ, γ-C$\underline{F}_2$), −123 (β-C$\underline{F}_2$), −126 (α-C$\underline{F}_2$). FTIR (KBr): 1717 (C=O$_{imide}$), 1784 (C=O$_{imide}$) cm^{-1}.

4.3.10. *Analytical data for 4-chloro-2-(4-n-tridecafluorohexylphenyl)isoindole-1,3-dione (**7**)*

Yield 1.15 g (66%), $t_r = 0.25$. ^{1}H NMR (CDCl$_3$) δ (ppm): 7.69 (m, 6H), 7.88 (t, 1H, $J = 4$ Hz). ^{13}C NMR (CDCl$_3$) δ (ppm): 122.5, 126.2, 127.2, 127.7, 128.4, 132.3, 133.6, 134.9, 135.6, 136.5, 164.3, 165.3. ^{19}F NMR (CDCl$_3$) δ (ppm): −81 (ω-CF3), −111 (ε-CF2), −122 (δ, γ-CF2), −123 (β-CF2), −127 (α-CF2). FTIR (KBr): 1721 (C=O$_{imide}$), 1776 (C=O$_{imide}$) cm^{-1}.

4.3.11. *Analytical data of 5-chloro-2-(4-n-tridecafluorohexylphenyl)isoindole-1,3-dione (**8**)*

Yield 1.66 g (96%), $t_r = 0.34$. ^{1}H NMR (CDCl$_3$) δ (ppm): 7.65 (d, 2H, $J = 9$ Hz), 7.73 (d, 2H, $J = 9$ Hz), 7.77 (dd, 1H, $J = 8$ Hz), 7.90 (d, 1H, $J = 9$ Hz), 7.94 (d, 1H, $J = 2$ Hz). ^{13}C NMR (CDCl$_3$) δ (ppm): 124.2, 125, 125.9, 127.7, 128.1. 129.3, 132.9, 134.6, 134.8, 141.4, 165.2, 165.5. ^{19}F NMR (CDCl$_3$) δ (ppm): −81 (ω-C$\underline{F}_3$), −111 (ε-C$\underline{F}_2$), −122 (δ, γ-C$\underline{F}_2$), −123 (β-C$\underline{F}_2$), −127 (α-C$\underline{F}_2$). FTIR (KBr): 1717 (C=O$_{imide}$), 1773 (C=O$_{imide}$) cm^{-1}.

4.3.12. *Analytical data for 4-bromo-2-(4-n-tridecafluorohexylphenyl)isoindole-1,3-dione (**9**)*

Yield 0.54 g (79%), $t_r = 0.14$. ^{1}H NMR (CDCl$_3$) δ (ppm): 7.70 (m, 5H), 7.93 (d, 2H, $J = 7$ Hz). ^{13}C NMR (CDCl$_3$) δ (ppm): 119.4, 123.1, 126.2, 127.8, 128.4, 129.0, 133.8, 135.0, 135.5, 139.7, 164.7, 165.1. ^{19}F NMR (CDCl$_3$) δ (ppm): −81 (ω-C$\underline{F}_3$), −111 (ε-C$\underline{F}_2$), −122 (δ, γ-C$\underline{F}_2$), −123 (β-C$\underline{F}_2$), −127 (α-C$\underline{F}_2$). FTIR (KBr): 1716 (C=O$_{imide}$) cm^{-1}.

4.3.13. *Analytical data for 5-bromo-2-(4-n-tridecafluorohexylphenyl)isoindole-1,3-dione (**10**)*

Yield 1.71 g (92%), $t_r = 0.41$. ^{1}H NMR (CDCl$_3$) δ (ppm): 7.64 (d, 2H, $J = 9$ Hz), 7.72 (d, 2H, $J = 8$ Hz), 7.82 (d, 1H, $J = 7$ Hz), 7.93 (dd, 1H, $J = 9$ Hz), 8.09 (d, 1H, $J = 1$ Hz). ^{13}C NMR (CDCl$_3$) δ (ppm): 125.4, 126.1, 127.4, 127.9, 128, 129.8, 130, 133.1, 135, 137.9, 165.4, 165.9. ^{19}F NMR (CDCl$_3$) δ (ppm): -81 (ω-C$\underline{F}_3$), -111 (ε-C$\underline{F}_2$), -122 (δ, γ-C$\underline{F}_2$), -123 (β-C$\underline{F}_2$), -127 (α-C$\underline{F}_2$). FTIR (KBr): 1717 (C=O$_{\text{imide}}$), 1769 (C=O$_{\text{imide}}$) cm^{-1}.

4.3.14. *Analytical data for 5,6-dichloro-2-(4-n-tridecafluorohexylphenyl)isoindole-1,3-dione (**11**)*

Yield 1.75 g (96%), $t_r = 0.48$. ^{1}H NMR (CDCl$_3$) δ (ppm): 7.63 (d, 2H, $J = 9$ Hz), 7.72 (d, 2H, $J = 9$ Hz), 8.04 (s, 2H). ^{13}C NMR (CDCl$_3$) δ (ppm): 125.9, 127.8, 130.4, 134.7, 139.8, 164.6, 186.4. ^{19}F NMR (CDCl$_3$) δ (ppm): -81 (ω-C$\underline{F}_3$), -111 (ε-C$\underline{F}_2$), -122 (δ, γ-C$\underline{F}_2$), -123 (β-C$\underline{F}_2$), -127 (α-C$\underline{F}_2$). FTIR (KBr): 1723 (C=O$_{\text{imide}}$), 1785 (C=O$_{\text{imide}}$) cm^{-1}.

4.3.15. *Analytical data for 4,7-dichloro-2-(4-n-tridecafluorohexylphenyl)isoindole-1,3-dione (**12**)*

Yield 1.67 g (91%), $t_r = 0.59$. ^{1}H NMR (CDCl$_3$) δ (ppm): 7.6–7.9 (m, 6H). ^{13}C NMR (CDCl$_3$) δ (ppm): 126.1. 127.6, 128.4, 130.6, 134.3, 137, 162.7. ^{19}F NMR (CDCl$_3$) δ (ppm): -81 (ω-C$\underline{F}_3$), -111 (ε-C$\underline{F}_2$), -122 (δ, γ-C$\underline{F}_2$), -123 (β-C$\underline{F}_2$), -127 (α-C$\underline{F}_2$). FTIR (KBr): 1716 (C=O$_{\text{imide}}$) cm^{-1}.

4.3.16. *Analytical data for 4,5,6,7-tetrachloro-2-(4-n-tridecafluorohexylphenyl)isoindole-1,3-dione (**13**)*

Yield 1.93 g (95%), $t_r = 0.37$. ^{1}H NMR (CDCl$_3$) δ (ppm): 7.62 (d, 2H, $J = 9$ Hz), 7.74 (d, 2H, $J = 8$ Hz). ^{13}C NMR (CDCl$_3$) δ (ppm): 126.0. 126.7, 127.7, 130.2, 134.0, 140.8, 161.8. ^{19}F NMR (CDCl$_3$) δ (ppm): -81 (ω-C$\underline{F}_3$), -111 (ε-C$\underline{F}_2$), -122 (δ, γ-C$\underline{F}_2$), -123 (β-C$\underline{F}_2$), -126 (α-C$\underline{F}_2$). FTIR (KBr): 1717 (C=O$_{\text{imide}}$) cm^{-1}.

K.J. gratefully acknowledges the Langley Aerospace Research Summer Scholar program sponsored by Hampton University. We thank C. Topping for performing DSC measurements, and Jirakorn Thisayukta at the University of North Carolina at Chapel Hill for help with the X-ray diffraction experiments. This research was supported by the National Aeronautics and Space Administration under NASA Contract No. NAS1-97046 while the author was in residence at ICASE, NASA Langley Research Center, Hampton, VA 23681-2199.

References

[1] Sasaki, S., and Nishi, S., 1996, *Polyimides*, edited by M. K. Ghosh, and K. L. Mittal (New York: Marcel Dekker), pp. 71–120.

[2] Eiselt, P., Denzinger, S., and Schmidt, H., 1995, *Liq. Cryst.*, **18,** 257.

[3] Bialecka-Florjańczyk, E., and Orzeszko, A., 2000, *J. mater. Chem.*, **10,** 1527.

[4] Berdaguè, P., Judeinstein, P., Bayle, J.-P., Nagaraja, C. S., Sinha, N., and Ramanathan, K. V., 2001, *Liq. Cryst.*, **28,** 197.

[5] Bunn, C. W., and Houwens, E. R., 1954, *Nature Lond.*, **174,** 549.

[6] Nguyen, H. T., Sigaud, G., Achard, M. F., Hardouin, F., Twieg, R. J., and Betterton, K., 1991, *Liq. Cryst.*, **10,** 389.

[7] Lobko, T. A., Ostrovskii, B. I., Pavluchenko, A. I., and Sulianov, S. N., 1993, *Liq. Cryst.*, **15,** 361.

[8] Ruhmann, R., Thiele, T., Wolff, D., Prescher, D., and Springer, J., 1996, *Liq. Cryst.*, **21,** 307.

[9] Neubert, M. E., 2001, *Liquid Crystals*, edited by S. Kumar (New York: Cambridge University Press), pp. 393–476.

[10] Soucy, C., Favreau, D., and Kayser, M. M., 1987, *J. Org. Chem.*, **52,** 129.

[11] Yoshino, N., Kitamura, M., Seto, T., Shibata, Y., Abe, M., and Keizo, O., 1992, *Bul. Chem. Soc. Jpn.*, **65,** 2141.